Shear-induced behavior in a solution of cylindrical micelles

M. Y. Lin,[1,*] H. J. M. Hanley,[2] S. K. Sinha,[1,3] G. C. Straty,[2] D. G. Peiffer,[1] and M. W. Kim[1]
[1]*Exxon Research and Engineering Co., Annandale, New Jersey 08801*
[2]*National Institute of Standards and Technology, Boulder, Colorado 80303*
[3]*Argonne National Laboratory, Argonne, Illinois 60439*
(Received 4 December 1995)

The structure of cylindrical aqueous micellar solutions was studied by small angle neutron scattering and light scattering in equilibrium and under shear. In equilibrium, the micelles behave as randomly oriented, rigid cylinders with an exponential distribution of lengths. Under an applied shear, the micelles generally align as expected, but at a particular concentration, close to the overlap concentration, applied shear has little effect until a threshold shear rate is reached and then only after a time delay. The results are consistent with some aspects of recent kinetic theories for the association and breaking of micelle systems under shear flow. [S1063-651X(96)50205-9]

PACS number(s): 64.70.Ja, 61.12.Ex, 64.60.Cn, 64.60.My

The structure of self-assembling systems and the various phases they exhibit have been the subject of much interest over the last several years [1]. In particular, surfactant molecules in aqueous solution display a rich variety of phenomena as they self-assemble to form micelles. The size, shape, and ordering of the micelles depend sensitively on parameters such as the surfactant concentration, the ionic concentration, and the temperature. Of particular interest are the tubular-cylindrical micelles, sometimes called ''living polymers'' [2]; their diameter is nearly constant but the length may vary, and the cylinders break and reform continuously. Solutions of these micelles are thus stable when subjected to high mechanical shears and their equilibrium properties recover when shear is removed. In this paper, we report small angle neutron scattering (SANS) and light scattering (LS) studies of these solutions, both in equilibrium and under shear. At a particular concentration (micellar volume fraction $\Phi=0.1\%$), we find an unusual threshold. Above the threshold the rod length increases with increasing shear and the rods become aligned. This finding is in contrast to those found at other concentrations, for which alignment is seen on immediate application of the shear.

The micellar solutions were prepared by mixing the surfactant, allylhexadecyldimethyl ammonium bromide, with an equal molar amount of sodium salicylate in D_2O [3]. The critical micellar concentration was determined by surface tension measurement to be approximately 0.002%, and viscosity data suggest an overlap concentration Φ^* near 0.15%. Neutron scattering data were taken at micellar concentrations $\Phi=0.02\%$, 0.1%, and 1.0%. The measurements were performed at the NG7-30m diffractometer at the NIST Cold Neutron Research Facility configured at a wavelength $\lambda=0.5$ nm and collected in a two-dimensional (2D) area detector. The magnitude of the scattering wave vector **Q** was within a range of 0.03 nm^{-1} to 1.5 nm^{-1} [$Q=(4\pi/\lambda)\sin\Theta$, where 2Θ is the scattering angle]. For the equilibrium runs, the solutions were placed in quartz cells with a path length of 5 mm between the two flat surfaces. For the shear studies, the samples were placed in a Couette shearing cell [4] with a 1 mm gap width. In Cartesian coordinates, the intensity is measured as a function of **Q** in the *xz* plane, with the neutron beam incident along the *y* axis. Under shear, the flow velocity (**u**) is in the *x* direction, the gradient is in the *y* direction, and hence the shear rate is defined as $\gamma=(\partial u_x/\partial y)$. All data were collected as 2D images and then circularly averaged or sector-averaged depending on whether anisotropy was observed in the patterns. Static light scattering data were taken on the nonsheared 0.1% solutions, using a laser of wavelength 514 nm and a photomultiplier mounted on a goniometer with the sample in a round quartz cell. All measurements were carried out at room temperture.

Figure 1 displays data obtained by both SANS and LS from the equilibrium 0.1% solution. There are three regimes: a small-Q regime ($Q\leqslant 0.01$ nm^{-1}, probed entirely with LS) where the flattening in $S(Q)$ arises because of the finite length of the micelles; an intermediate Q regime ($0.01\ nm^{-1}\leqslant Q\leqslant 0.6\ nm^{-1}$) where $S(Q)$ varies as Q^{-1}, corresponding to randomly oriented stiff rods [5]; and a rolloff to the Porod regime due to their finite radius ($Q\geqslant 0.6$ nm^{-1}). The intensity $S(Q)$ was fitted with a model of randomly oriented cylinders [5] where

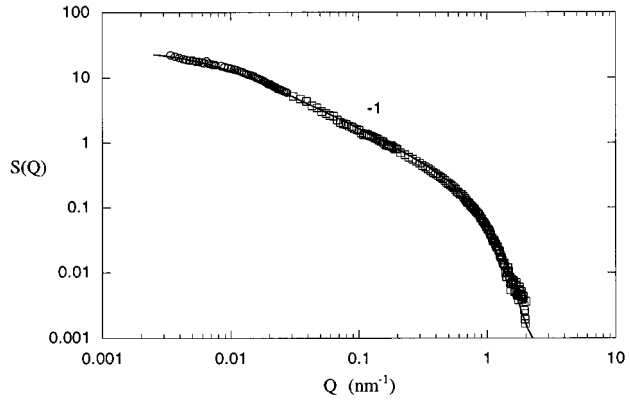

FIG. 1. SANS (squares) and LS (circles) data for the 0.1% solution at equilibrium. The solid line is a fit of randomly oriented cylinders with an average half length of 115 nm and an average radius of 1.7 nm. In this logarithmic plot, the intermediate region has a slope of ~ -1, characteristic of randomly oriented long rods.

*Present address: National Institute of Standards and Technology, React E151, Gaithersburg, MD 20899.

$$S(Q)=\langle S(Q)_{l,a}\rangle=A\int_0^{\pi}p(\beta)\langle F^2(Q,\beta)\rangle\sin\beta\ d\beta. \quad (1)$$

The factor A is a product of an instrumental constant, the concentration of surfactants, the micellar aggregation number, and the square of the scattering length density contrast between the micelle and the solvent. The form factor for a rod of radius a and half length l, and oriented in a direction which is an angle β from the vector $\mathbf{Q}$ is

$$F(Q,\beta)=\frac{\sin(Ql\ \cos\beta)}{Ql\ \cos\beta}\frac{J_1(Qa\ \sin\beta)}{Qa\ \sin\beta} \quad (2)$$

where $J_1(x)$ is the first order Bessel function of the first kind. The term $p(\beta)$ is the rod orientation probability which, in the equilibrium case, is independent of β. The brackets $\langle\ \rangle$ in Eq. (1) denote an average over both l and a. For the length, we use the well-known exponential form for living micelles [6] given by

$$N(l)=\begin{cases}0, & l<l_0\\ N_0\exp(-l/L), & l\geq l_0\end{cases} \quad (3)$$

where $N(l)$ is the number density of micelles of half-length l, and l_0 is a low-l cutoff (minimum length) value, N_0 is a constant, and L is the average half-length. The data were fitted using Eqs. (1)–(3), treating L, l_0, N_0, and a as variables (the radius a was averaged over a Shultz distribution with a standard deviation of 25%). Figure 1 shows that such a model provides a good representation of the data over three decades of Q. The fits yielded $L=115$ nm and $l_0=a=1.7$ nm.

Only SANS measurements were performed for the 0.02% and 1.0% solutions. These intensities all scale with that of the 0.1% sample, suggesting that the micelles' stiffness (Q^{-1} behavior) and their radii are independent of the concentration. Even though the Q range of SANS is not small enough to probe $1/l$, we can still obtain L for the other two samples based on the amplitude of their scattering intensity. This amplitude scales as ΦLa^2. Since a is nearly a constant, knowing L for the $\Phi=0.1\%$ sample, and Φ for the other two samples, we obtain the length $L=85.6$ nm for the 0.02% solution and 117 nm for the 1.0% solution (some evidence of intermicellar interactions was apparent at $Q<0.01$ nm^{-1} for the 1.0% sample, therefore we determine the amplitude using only the data of $Q>0.1$ nm^{-1}).

The data taken under shear were analyzed in the context of the formalism of Hayter and Penfold [7]. These authors define the probability $p(\beta)\equiv p(\theta,\phi;P)$ in terms of the Péclet number, $P=\gamma/D_r$. The Péclet number is the ratio of two competing rates: the shear rate γ, which is the rate of the alignment of the rod in the flow direction, and a randomizing rate assumed to be the rotational diffusion coefficient, D_r. The probability is given by

$$p(\theta,\phi;P)=\frac{(1-\cos2\phi_0)(1+\sin^2\theta\ \cos2\phi_0)^{3/2}}{4\pi[1-\sin^2\theta\ \cos\phi_0\cos2(\phi-\phi_0)]^2} \quad (4)$$

where Hayter and Penfold define $2\phi_0=\tan^{-1}(8/P)$ through which the probability depends on P. The scattering intensity is then

$$S(\mathbf{Q})=\langle S(\mathbf{Q})_{l,a}\rangle=\langle S(Q,\varphi)_{l,a}\rangle$$
$$=A\int_0^{2\pi}d\phi\int_0^{\pi}\sin\theta\ d\theta\langle p(\theta,\phi;P)F^2(Q,\beta)\rangle. \quad (5)$$

In Eq. (5) φ is the angle between the wave vector $\mathbf{Q}$ and the horizontal axis (x axis) of the area detector, and the relationship between β and the polar coordinates and φ is

$$\cos\beta_{\pm}=\sin\theta\ \cos\phi\ \cos\varphi\pm\cos\theta\ \sin\varphi. \quad (6)$$

[The two signs occur because the beam traverses the sample twice in the shear cell, with the flow direction reversed in the two regions. Thus $F^2(Q,\beta)$ is equivalent to $F^2(Q,\beta_+)+F^2(Q,\beta_-)$.] In this formalism, the interactions between rods, such as collisions and other effects, are not taken into account. Nevertheless, the formalism can provide a good representation of our data if D_r is defined to be

$$D_r=\frac{3k_BT}{8\pi\alpha\eta l^3}\{\ln(2l/a)-1.57+7[0.28-1/\ln(2l/a)]^2\} \quad (7)$$

which differs from the original Hayter-Penfold expression [7,8] by a factor α. This factor modifies the solvent viscosity η to an ''effective viscosity'' $\alpha\eta$ to include the effects of interactions. Alternatively, this modification can also be seen as to change P to αP, while keeping the original definitions of D_r and η intact, as discussed later.

Intensities from the nonequilibrium runs were fitted using Eqs. (2)–(7), where α is the additional variable. The fitting procedure was carried out as before. For computational rea-

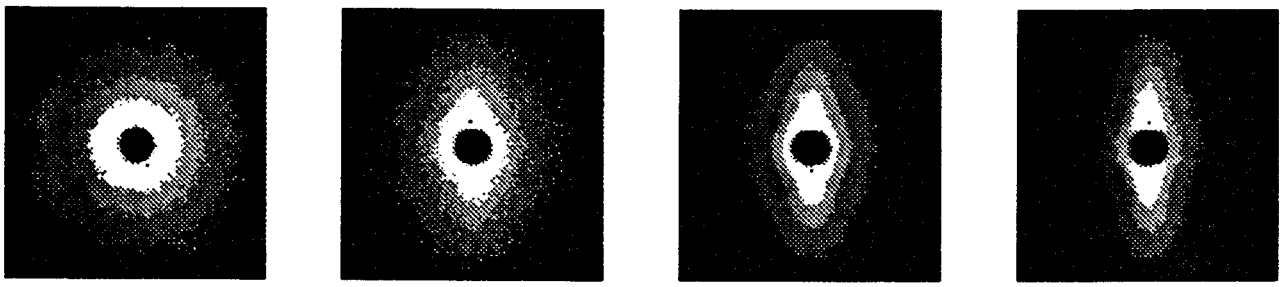

FIG. 2. Two-dimensional scattering patterns of the SANS data of the 0.1% solution evolving as the shear rate increases (from left to right, the shear rates are $\gamma=30$, 40, 65 and 80 s^{-1}). The shear flow is on the horizontal direction ($\varphi=0$). Above $\gamma=80$ s^{-1}, the pattern changed very little. The Q range of the patterns is from 0.15 nm^{-1} (near the beam stop) to 1.2 nm^{-1} (at the corners).

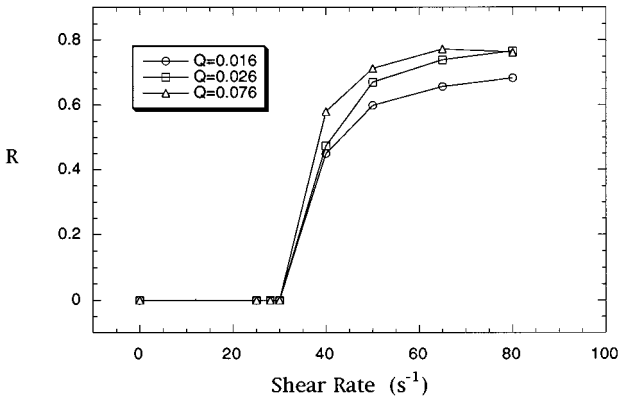

FIG. 3. Anisotropy ratio defined as $R=[S(Q,\varphi=90°)-S(Q,\varphi=0°)]/S(Q,\varphi=90°)$ for three different Q values. It is striking to see that the ratio is zero until some threshold shear rate ≈ 40 s^{-1} is reached. The ratio also appears to saturate at $\gamma \geqslant 80$ s^{-1}.

sons, however, we ignored polydispersity in the radius a. We have further assumed implicitly that the length distribution of the micelle rods is *independent* of their orientations, which greatly simplifies the analysis.

Results for the 0.02% concentrations solution under shear can be fitted with the above model with α of Eq. (7) set equal to 1. We found typically that L increased from the equilibrium value of 85.6 nm to 145 nm at $\gamma=100$ s^{-1} ($P=0.73$). The results are consistent with those expected from a dilute solution, containing relatively collision-free rods; the shear flow has induced both partial orientation and length growth. Data from the 1% solution subjected to shear showed a distinctive ''butterfly'' pattern in $S(\mathbf{Q})$ which is not yet understood and will be the subject of future work.

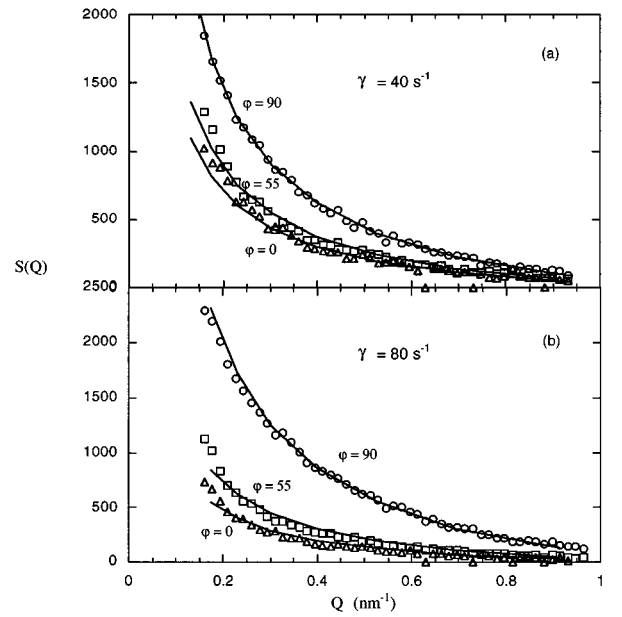

FIG. 4. Data from the 0.1% solution fitted using the modified Hayter-Penfold formalism at (a), $\gamma=40$ s^{-1}, just above the threshold shear rate and after the delay time; and (b), at $\gamma=80$ s^{-1}. Points represent the data at angles φ as labeled. The lines are calculated. (Deviations of the data from the fits for $\varphi=0°$ and $\varphi=55°$ at very low Q are due to the poor resolution in φ.)

TABLE I. Parameters for the 0.1% concentration micellar solution.

γ (s^{-1})	a (nm)	L (nm)	l_0 (nm)	α	C	P
0	1.7	115	1.7		0.73	0
40	2.27	165	49	1.75	1.50	0.42
50	2.38	222	112	2.05	2.72	1.16
65	2.38	210	111	2.48	2.42	1.30
80	2.34	213	118	2.28	2.49	1.66

The results for the 0.1% solution are of particular interest here. Figure 2 displays the 2D patterns for $S(\mathbf{Q})$ as a function of shear. The novel result observed was that anisotropy due to alignment was not evident until a threshold shear rate $\cong 40$ s^{-1} was reached, and then only after a time delay of 7 to 8 min after the shear was applied. For $\gamma > 40$ s^{-1} the pattern slowly evolves to yield more anisotropy as the shear rate increases, but no detectable time delay was observed [9]. No substantial changes were seen for $\gamma \geqslant 80$ s^{-1}. Figure 3 plots the anisotropy ratio of $S(\mathbf{Q})$ as a function of γ, showing clearly the transition at the threshold shear rate. Data taken from the samples at 0.02% and 1.0% at even a wider shear rate range, however, did not display this apparent threshold shear or delay time. Therefore, flow instability or temperature variation inside the sheared fluid and other external conditions as possible causes for the threshold is ruled out.

Figure 4 shows typical cuts of the data at $\varphi=0°$, 55°, and 90° for applied shear rates of 40 s^{-1} (taken after the delay time) and 80 s^{-1}, together with the fits according to the modified Hayter-Penfold model. The model, with the exponential length distribution and parameter α, represents the data well at all shear rates. Due to the additional parameter φ in the anisotropic scattering pattern, SANS can be sensitive to a longer length scale than in the case of isotropic scattering. Table I lists the parameters L, l_0, a, and α. The key results are as follows: (1), above the threshold shear rate, $\gamma=40$ s^{-1}, L increases to and saturates at about twice its equilibrium value, but a remains constant (the slightly larger value of the cylinder radius obtained from the shear data is a consequence of neglecting the polydispersity in the later fits and is not regarded as significant); (2), for shear rates above the threshold, the factor α increased to a value slightly above 2, implying a greater degree of alignment than expected from the Hayter-Penfold theory, even allowing for an increase in the rod lengths.

The $\Phi=0.1\%$ solution is sufficiently dilute that no nematic order can exist in the absence of shear (nematic order has been observed in dense solutions of similar micelles [10,11].) For dilute solutions, however, experiments by Rehage, Wunderlich, and Hoffmann showed a dramatic rise in viscosity at a critical shear rate [12]. Their results led Bruinsma *et al.* [13] to propose a kinetic theory for rodlike aggregation of tubular micelles under shear. Bruinsma *et al.* have different solutions for the average rod length according to regimes characterized by two parameters, the Péclet number P and the dimensionless concentration $C=\Phi_L L^3$, where Φ_L is the micelle number density [alternatively $C=\Phi(L/a)^2/2\pi$]. For $C<1$, they find L increases slightly with shear for $P \geqslant 1$. Data from our 0.02% solution, for which $0.08 \leqslant C \leqslant 0.23$ with $P=0.78$ at $C=0.23$, are consistent with their findings. For $C \geqslant 1$, characterized as a fast reaction

regime—for which many inter-rod collisions occur before a rod has had significant time to rotate—they find the following: for $P<1$, a metastable solution with a mean rod size $L \approx L^{(0)}$, the equilibrium value; for $P>1$, a runaway solution for which the mean rod length diverges. For our experiments, at $\Phi=0.1\%$, $C=0.73$ at equilibrium and $C>1$ for the system under shear (Table I). If $P=1$ corresponds to the threshold shear, our results are consistent with this aspect of the theory, except that we do not observe a true divergence of L with shear. The reason for this discrepancy may be that Bruinsma *et al.* have assumed that the rods are flexible, and that rod combination results every time two rods collide even if noncollinear, while breakage is caused by the velocity gradient along the rod, which is independent of the collision rate. This mechanism inevitably will cause the length to diverge since in the fast reaction regime the collision rate is very high. In any case, their theory is inapplicable for a system sheared above the threshold, because their simplifying assumption of random rod orientations even under high shear cannot generally be valid and is contrary to our data.

Turner and Cates [14] also addressed the experimental data of Rehage *et al.*, but their theory assumes that the rods are stiff and only collinear collisions will result in rod combination, which appears to be a valid assumption in the case of our system. According to their predictions, the rod length will sharply increase but not diverge. They also predict, but do not calculate explicitly, an anisotropy in the orientational distribution of the rods under shear. However, these authors do not predict a threshold for the shear rate at which the rod length begins to increase or at which the rods begin to align, as observed here.

We may speculate on the existence of shear threshold and the related time delay for the micellar alignment using concepts embodied in the above approaches. The dimensionless concentration C may also be written as the ratio J_s/γ, where J_s is the rate of collision due to shear ($J_s=\gamma\Phi_L L^3$). If $C \geqslant 1$, as in the fast reaction regime and the rods are initially directionally random, it is difficult for alignment to be established due to the rapid random collisions. If the rods are stiff, rod combination and growth are largely inhibited. If however, a certain degree of alignment can be established, given a sufficient *time* or *rate of shear*, the probability of combination increases because collinear collisions become more probable. Also, after the micelles become aligned, the effect of intermicellar collision is just the opposite from before: collisions prevent the rods from being randomized again. Since most of them are aligned, a collision with the neighboring micelles will most probably kick a micelle back to the original, aligned direction. Thus a cooperative balance for both rod length increase and rod orientation will occur. The ''effective'' Péclet number in the orientational distribution [Eq. (4)] then becomes the ratio of the rate of collisions due to shear (thus the rate plays the role of the alignment rate instead of γ) to D_r, the rate of misalignment due to rotational diffusion. Thus $P_{\rm eff}=P(J_s/\gamma)=PC$. From Eq. (7), we see that an alternative way to represent this ''effective'' Péclet number is to use the actual P, but with an effective solvent viscosity $\eta_{\rm eff}=C\eta$. Hence the fitting parameter α used with Eq. (7) should be equal to the dimensionless concentration C, and indeed they are almost identical as seen in Table I.

In summary, we have studied SANS from a system of cylindrical micelles subjected to various degrees of shear. For the 0.1% solution—which is just below the overlap concentration—we apparently have two phases: a frustrated phase when the shear rate is low and the micelles appear to be randomly oriented, as suggested by the isotropic pattern of the scattering, and an aligned phase at higher shears, when the scattering pattern is anisotropic. The border between the two phases is characterized by a ''threshold'' shear rate. The initial phase apparently flips over to the second phase after a time delay (7–8 min in our experiments). We speculate that below the threshold shear, collisions between randomly oriented micelles, and therefore lack of collinear combination reactions inhibit the micelle growth and alignment, a state similar to the metastable state Bruinsma *et al.* described. Once the shear rate is high enough, however, an energy barrier is overcome, so most of the micelles do indeed become aligned. Once the micelles are aligned, collisions tend to keep the alignment in place. It is this highly nonlinear effect of the shear-induced collisions which is responsible for the apparent phase transition. Whether this phase transition is associated with the overlap concentration will be the subject of future work.

We thank S. Milner, E. Herbolzheimer, J. Penfold, and S.-H. Chen for many useful discussions. One of us (M.Y.L.) wants to thank A. Krall and D. Weitz for helping setting up the light scattering experiment. The NIST contribution to this work was supported in part by Air Force of Scientific Research Grant No. AFOSR-MIPR-94-0027.

[1] *Micellar Solutions and Microemulsions*, edited by S.-H. Chen and R. Rajagopalan (Springer-Verlag, New York, 1990); *Micelles, Membranes, Microemulsions, and Monolayers*, edited by W. M. Gelbert *et al.* (Springer-Verlage, New York, 1992).
[2] X.-l. Wu *et al.*, Phys. Rev. Lett. **68**, 1426 (1992).
[3] D. G. Peiffer, J. Poly. Sci. Part A **28**, 619 (1990).
[4] G. C. Straty, Natl. Inst. Stand. Technol. J. Res. **94**, 351 (1989); G. C. Straty, J. Stat. Phys. **62**, 1015 (1991).
[5] See, for example, G. Porod, in *Small Angle X-ray Scattering*, edited by O. Glatter and O. Kratky (Academic Press, New York, 1982).
[6] T.-L. Lin *et al.*, J. Phys. Chem. **91**, 406 (1987).
[7] J. B. Hayter and J. Penfold, J. Phys. Chem. **88**, 4589 (1984).
[8] S. Broersma, J. Chem. Phys. **32**, 1626 (1960).
[9] More recent experiments using much smaller time resolution in $S(\mathbf{Q})$ showed that time delays ranging from 5 to 30 s are present for shear rates above the threshold.
[10] V. Shmitt *et al.*, Langmuir **10**, 955 (1994).
[11] V. K. Jindal *et al.*, J. Phys. Chem. **94**, 3129 (1990).
[12] H. Rehage *et al.*, Prog. Coll. Poly. Sci. **72**, 51 (1986).
[13] R. Bruinsma *et al.*, J. Chem. Phys. **96**, 7710 (1992).
[14] M. S. Turner and M. E. Cates, J. Phys. Condens. Matter **4**, 3719 (1992).